Changeover from glassy ferromagnetism of the orbital domain state to long-range ferromagnetic ordering in $La_{0.9}Sr_{0.1}MnO_3$

K. Mukherjee and A. Banerjee
UGC-DAE Consortium for Scientific Research, University Campus, Khandwa Road, Madhya Pradesh, Indore 452017, India
(Received 10 May 2007; published 31 January 2008)

An attempt is made to resolve the controversy related to the low temperature phase (ground state) of the low-doped ferromagnetic (FM)-insulator manganite through bulk magnetic measurements on $La_{0.9}Sr_{0.1}MnO_3$ sample. It is shown that the FM phase, formed out of well defined transition in the low-doped system, becomes inhomogeneous with decrease in temperature. This inhomogeniety is considered to be an outcome of the formation of orbital domain state of e_g electrons having hole rich (metallic) walls separating the hole deficient (insulating) regions. The resulting complexity brings in metastability and glassy behavior within the FM phase at low temperature, however, with no resemblance to spin glass, cluster glass, or reentrant phases. It shows aging effect without memory but magnetic relaxation shows signatures of intercluster interaction. The energy landscape picture of this glassy phase is described in terms of hierarchical model. Further, it is shown that this inhomogeneity disappears in $La_{0.9}Sr_{0.1}MnO_{3.08}$ where the orbital domain state is destroyed by self-doping, resulting in reduction of Mn^{3+} and hence e_g electrons. The ferromagnetic phase of the nonstoichiometric sample does not show glassy behavior. It neither follows "hierarchical model" nor "droplet model" generally used to explain glassy or inhomogeneous systems. Its magnetic response can be explained simply from the domain wall dynamics of otherwise homogeneous ferromagnet.

DOI: 10.1103/PhysRevB.77.024430 PACS number(s): 75.47.Lx, 75.60.Ch, 76.60.Es

I. INTRODUCTION

The physics controlling the properties of low-doped manganites is a subject of intense research currently due to the fact that magnetic ground state of these compounds continues to be a subject of controversy.[1–10] The physical properties exhibited by these compounds are likely to be proximate to those of other low-doped transition metal oxides, such as cuprates and nickelates. Lightly doped manganites show ferromagnetic insulating behavior inspite of finite amount of hole doping, indicating that these transition metal oxides (TMOs) belong to a class of strongly correlated electron system and the effect of correlation among the electrons prevents the ground state from being metallic. Introduction of holes in these systems results in inhomogeneity, which divides the system into different regions having varying hole densities. Generally, in these systems, the kinetic and potential energies are of the same energy scale and incorporation of Coulomb interaction in these regimes leads to various self-organized structures, with clusters of one phase embedded in the other, a phenomenon referred as electronic phase separation (EPS).[11] Recent theoritical studies also highlight the role of Coulomb interaction in studying the electronic inhomogeneity in manganites.[12] EPS either results in formation of regions having competing magnetic interactions or in self-generated clusters, interaction among which results in blocking[13] or freezing mechanism (observed generally in TMO) at certain temperatures. Studies on cuprates[14,15] and nickelates[16] have revealed a microscopic segregation of doped holes in antiferromagnetic phase into walls leading to an ordering consisting of charged domain walls that forms antiphase boundaries between antiferromagnetic domains. Studies by Tranquada *et al.* on $La_{1.48}Nd_{0.4}Sr_{0.4}CuO_4$ (Ref. 17) and $La_{1.69}Sr_{0.31}NiO_4$ (Ref. 18) have revealed stripe phase order of hole and spins. $La_{0.9}Sr_{0.1}MnO_3$ with $x=0.1-0.17$ belong to the class of compound known as ferromagnetic insulator (FI). The self-organized regime observed in nickelates and cuprates is also expected in FI phase of manganite. Recent theories[19] and experiments[10] have provided evidences that orbital ordering (OO) plays an important role along with spin and charge in the insulating state of low-doped manganites by controlling the e_g electron mobility. Experimental results on $La_{0.88}Sr_{0.12}MnO_3$ (Ref. 4) indicates the transition between two ferromagnetic phases, one metallic and another insulating driven by orbital ordering. It has been proposed that the OO phase might contain ferromagnetic insulating domains separated by ferromagnetic metallic walls,[7] which raises question of stripes formation in the ferromagnetic insulating phase.[20]

Temperature dependence of ac susceptibility and low field magnetization of low-doped $LaMnO_3$ shows interesting magnetic behavior. Urushibara *et al.*[21] showed that $La_{0.9}Sr_{0.1}MnO_3$ is orthorhombic and undergoes a paramagnetic to ferromagnetic transition followed by a transition at low temperature accompanied with insulating behavior. Susceptibility of ferromagnets generally varies as the inverse of demagnetization factor and is expected to be constant at low temperature in the absence of any further magnetic transition. Studies of the critical regimes in $La_{0.875}Sr_{0.125}MnO_3$ revealed that the paramagnetic to ferromagnetic phase transition is accompanied by consistent critical exponents belonging to three-dimensional (3D) Heisenberg universality class.[22] However, the low temperature transition which received considerable attention in the past decade remains undetermined. The nature of this low temperature phase previously has been interpreted in terms of canted antiferromagnetic phase.[1] Successive structural phase transition from a high temperature pseudocubic phase to intermediate Jahn-Teller distorted orthorhombic phase and to low temperature pseudocubic phase reported in this low-doped

regime[23,24] might be a cause of the observed behavior. The nature of low temperature state is also reported in terms of charge localization, which is accompanied by ordering of polarons.[2] A field induced phase transition from a ferromagnetic metallic phase to a ferromagnetic insulating phase as reported in $La_{0.875}Sr_{0.125}MnO_3$ (Ref. 3) might be responsible for the observed low temperature phenomenom. The low temperature fall in magnetization in $La_{0.9}Ca_{0.1}MnO_3$ is intrepreted in terms of domain wall pinning effect by Joy and Date.[5] The two successive transitions with the lowering of temperature can be due to reentrant spin glass transition.[25] Recent studies from neutron diffraction, small angle neutron scattering, and nuclear magnetic resonance show that the ground state of $La_{0.9}Ca_{0.1}MnO_3$ consists of disordered double exchange metallic clusters that coexists with long range superexchange based ferromagnetic insulating regions.[6] Hence, the above reports show a wide variety of possibilities of the low temperature phase and ground state of such low-doped FI manganites.

In manganites, the ratio of Mn^{3+}/Mn^{4+} and their distribution in the lattice plays an important role in tuning the physical properties of these systems. Generally, the amount of Mn^{4+} is tuned by divalent cation doping on *A* site of perovskite structure but its amount can also be increased by oxidation of the stoichiometric sample resulting in a change of physical properties of the compound arising out of nonstoichiometry. The excess oxygen is accounted by an equal number of vacancies at *A* and *B* sites of ABO_3 perovskites, while the oxygen network in believed to be undefected.[26] As said earlier, investigations of low-doped manganites have revealed the formation of orbital domain state in the ferromagnetic insulating regimes.[7,10] Increasing nonstoichiometry increases the Mn^{4+} content, resulting in suppression of the OO phase with the clusters becoming more populous eventually coalescing leading to the establishment of homogeneous ferromagnetic order. Hence, the metamagnetic behavior of the OO phase is expected to decrease with the increasing nonstoichiometry. Such stoichiometry dependent behavior is also observed in other transition metal oxides such as cuprates[15] and cobaltates[27] and more recently in bilayered manganite.[28]

In this paper, through bulk magnetization, we investigate the magnetic ground state of stoichiometric $La_{0.9}Sr_{0.1}MnO_3$, as its true nature is in the center of debate. A detailed investigation of the effect of both ac and dc magnetic fields on the physical properties of this compound indicates that the observed low temperature behavior is not because of magnetic transition but due to the development of an inhomogeneous phase with the reduction in temperature. The resulting self-organized regimes are of the form of orbital domains, dictated by OO, which plays an important role in defining the ground states of the compound. Increase of disorder (in form of self-doping) suppresses the orbital domain state and a homogeneous ferromagnetic ordering is observed. The magnetic behavior of the resulting nonstoichiometric compound is ascribed to domain wall dynamics in a ferromagnetic matrix, whereas the orbital domains of the stoichiometric sample show glassy ferromagnetic behavior with the glassiness arising solely due to intercluster interaction. The results are also compared with the hierarchical model.

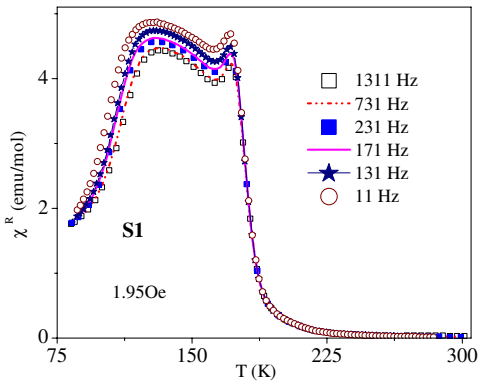

FIG. 1. (Color online) Frequency dependence of real part of ac susceptibility (χ^R) of S1 sample.

II. SAMPLE PREPARATION AND CHARACTERIZATION

Two polycrystalline sample $La_{0.9}Sr_{0.1}MnO_3$ (S1) and $La_{0.9}Sr_{0.1}MnO_{3.08}$ (S2) has been prepared by standard solid-state ceramic route with starting materials having purity of >99.9%. Stoichiometric proportions of the starting materials La_2O_3, Sr_2CO_3, and MnO_3 were mixed and heated in air at 950 °C for 24 h twice. After grinding the powder, pellets were made and given a heat treatment of 1250 °C. For sample S1, the final sintering is given at 1400 °C. Then, it is annealed under nitrogen atmosphere for 36 h. Sample S2 is annealed under oxygen atmosphere for 24 h after the final sintering at 1250 °C. X-Ray diffraction (XRD) was carried out using Rigaku Rotaflex RTC 300 RC diffractometer with Cu $K\alpha$ radiation. The collected XRD pattern is analyzed by the Rietveld profile refinement using the profile refinement program by Young *et al.*[29] Estimation of Mn^{3+}/Mn^{4+} is done by iodometric redox titration using sodium thiosulphate and potassium iodide. ac susceptibility and dc magnetization are done using a homemade ac susceptometer[30] and a vibrating sample magnetometer.[31]

Samples S1 and S2 crystallize in orthorhombic (*Pbnm*) and rhombohedral structure ($R\bar{3}c$), respectively. The samples are seen to be single phase with the goodness of fit around 1.2 for both cases. For S1, the percentage of Mn^{3+} and Mn^{4+} is, respectively, about 89% and 11%, while that for S2 is 74% and 26%, respectively.

III. RESULTS AND DISCUSSIONS

A. Realization of orbital domain state in stoichiometric (S1) sample

Figure 1 shows the frequency dependence of real part (χ^R) of ac susceptibility. The fall in susceptibility at lower temperature is also observed when measurement are done on a single crystals of $La_{0.9}Sr_{0.1}MnO_3$ and $La_{0.875}Sr_{0.125}MnO_3$.[22] The temperature variation of χ^R shows paramagnetic to ferromagnetic transition around 175 K followed by a hump and the imaginary part (χ^I) also shows a peak and a fall at lower temperature. ac-χ is seen to be frequency dependent below T_c with χ^R decreasing as frequency is increased, normally observed in metastable system such as spin glasses, cluster

glasses, superparamagnets, reentrant systems, etc. However, there is no shift in temperatures of the peaks with frequency for χ^R and χ^I. A frequency dependent peak, which shifts toward higher temperatures with increasing frequency, is a characteristic features of the dynamics of spin glass system and is also observed in other manganite samples which shows cluster glasslike behavior.[32] This observation rules out any spin glasslike dynamics, superparamagnetic, or cluster glass-type behavior in the low temperature region.

Reports in literature[23] shows the presence of a low temperature structural transition in this compound. This results in changed occupancy of orbitals by e_g electron due to the change of lattice constant, leading to the reformation of domains with larger number of domain walls. Sr^{2+} substitution results in inhomogeneous distribution of Mn^{3+} and Mn^{4+} with Mn^{4+} concentration around the divalent ion,[33] resulting in the formation of clusters. These clusters break into smaller pieces due to low temperature structural transition leading to segregation of charge, making the low temperature phase inhomogeneous. The reformation of domains taking place leads to enhanced wall number, which are pinned to the new structure. Hence, the dynamic response of the spin decreases with decreasing temperature, as the low field is not sufficient to activate the pinned walls resulting in the observed fall in susceptibility. Hence, the resulting self-organized regimes in the form of clusters of various sizes make the low temperature region of the sample metastable.

To further emphasize the fact that magnetic transition is absent in the low temperature region, thermal cycling in both ac and dc magnetizations is done. The presence of thermal hysteresis is a general phenomenon associated with first order phase transition (FOPT). The susceptibility curve both (χ^R and χ^I) does not show thermal hysteresis around the region where the fall in observed [Fig. 2(a) and its inset]. Figure 2(b) show field cooled cooling (FCC) and field cooled warming (FCW) cycles of dc Magnetization. Unlike the zero field cooled magnetization (ZFCM) case, the field cooled magnetization rises continuously with decreasing temperature. The graph also shows the absence of thermal hysteresis throughout the temperature range between FCC and FCW. These observations rule out any ferromagnetic to antiferromagnetic FOPT in the low temperature region of the compound. To substantiate the above fact, magnetocaloric effect (MCE) measurement is done on the sample [shown in inset of Fig. 2(b)]. The entropy change, calculated from the *MH* isotherm at different temperatures, shows a peak around T_c with the absence of any significant peak a lower temperature region. This also indicates the absense of ferromagnetic (FM)-antiferromagnetic (AFM) transition at lower temperature as a peak in MCE is expected around the transition. Hence, the low temperature phase, as seen from thermal hysteresis in magnetization and MCE measurement, is different from the metastable state arising from standard first order transition between competing ferromagnetic and antiferromagnetic phases where near the transition a short-range correlation of one of the two phases starts building up at the cost of other.

Hence, the above measurements indicate the absence of antiferromagnetic transition, spin glass dynamics, or cluster glasslike behavior in the low temperature region and brings

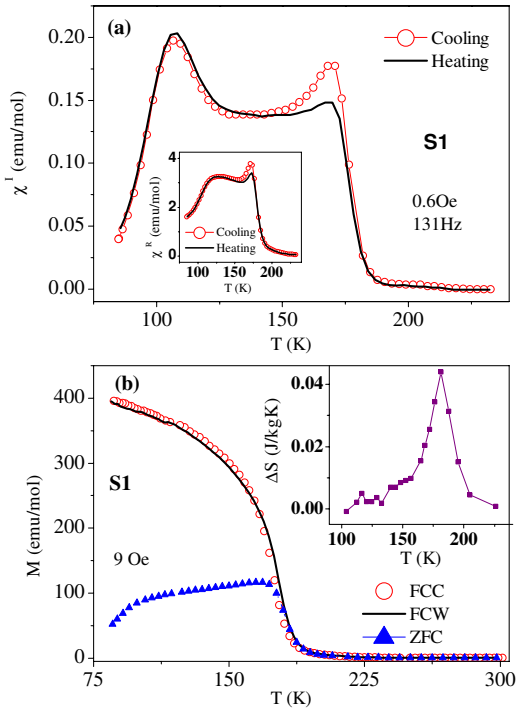

FIG. 2. (Color online) (a) Thermal hysteresis (TH) imaginary part of ac susceptibility (χ^I) of S1 sample. Inset shows TH of the real part of ac susceptibility (χ^R). (b) Temperature response of field cooled warming (FCW) and field cooled cooling (FCC) curves of dc magnetization along with zero field cooled magnetization (ZFCM) curve at 9 Oe of S1 sample. Inset shows temperature dependence of magnetocaloric effect of the same.

out the novel role of orbitals for explaining the observed features of the sample. The presence of low temperature structural transition in this compound leads to orbital rearrangement, resulting in orbital degree of freedom of e_g electrons playing the central role in defining the ground state properties. So, the absence of antiferromagnetic state along with the insulating behavior of the transport, which shows a slope change around T_c (Ref. 21) (due to decrease in the value of resistivity), indicates the coexistence of ferromagnetic metallic and ferromagnetic insulating phase at low temperatures. The insulating behavior of the ferromagnetic phase is explained in terms of antiferro-type orbital ordering, which leads to elongation and compression of the neighboring MnO_6 octahedrons, resulting in unequal Mn-O bond distances. According to Goodenough's theory of semicovalence,[34] the magnetic coupling will be ferromagnetic when the Mn-O bonds are semicovalent, leading to ferromagnetic superexchange interaction. Such type of magnetic coupling in similar compounds is also reported in literature.[3,4,35] Hence, the low temperature phase is an electronically and hence magnetically inhomogeneous state consisting of hole poor and hole rich regions. So, an orbital domain state with ferromagnetic insulating domain separated by ferromagnetic metallic wall as observed from NMR measurements in $La_{0.8}Ca_{0.2}MnO_3$ (Ref. 7) is also realised in our case.

Orbital domains realized in the sample make the low temperature region metastable, resulting in a nonequilibrium

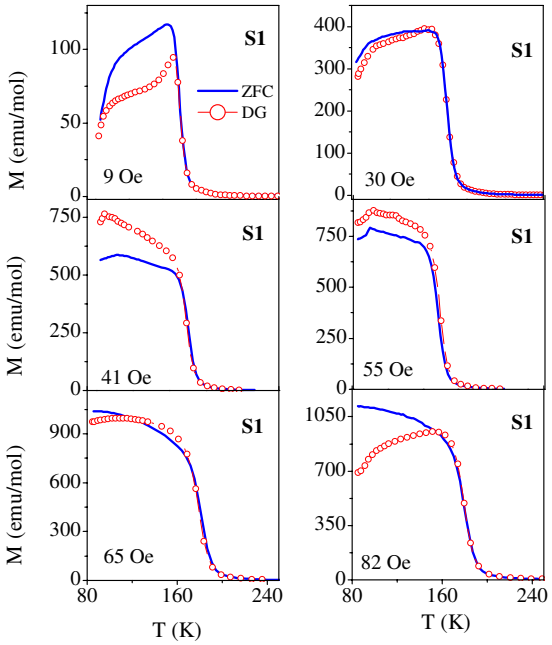

FIG. 3. (Color online) Temperature response of magnetization after zero field cooling (ZFC) (line) and applying a field and degaussing the ZFC sample (DG) (open circles) at different magnetic fields for S1 sample.

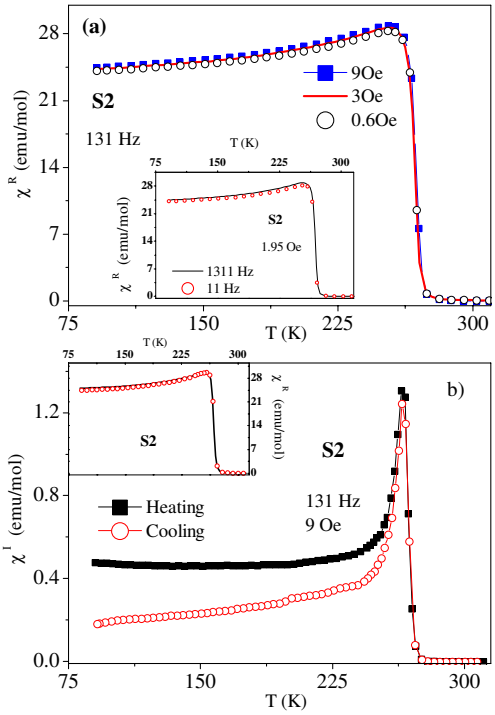

FIG. 4. (Color online) (a) Field dependence of real part of ac susceptibility (χ^R) of S2 sample. Inset shows frequency dependence of real part of ac susceptibility (χ^R) of the same. (b) Thermal hysteresis (TH) of the imaginary part of the ac susceptibility (χ^I) for S2 sample. Inset shows the TH of real part of ac susceptibility (χ^R).

state where reformation of domains takes place. To probe the energy landscape in this region, degaussing (DG) experiment[5] is done at different dc fields. Such demagnetization based studies are considered to give a systematically better approximation of the ground state of disordered systems, as reported in Ref. 36. In DG measurements, after ZFC to 85 K, 1000 Oe field is applied and then it is reduced to zero. Application of the field disturbs the ground state spin arrangement and results in some remanent magnetization. The remanent magnetization is reduced to zero by repeated field cycling with reducing amplitude (degaussing). Then, the measuring field is applied at 85 K and temperature response of magnetization is noted while warming. Figure 3 shows the M-T curves in different measuring fields for degaussed, as well as the corresponding ZFC states. At 9 Oe, the degaussed curve obtained below the normal ZFC curve, while for 30 Oe, the bifurcation between the curves reduces. At 41 Oe, the DG curve is above the normal ZFC curve. Again, the seperation between the curves decreases at 55 Oe and there is a crossover at 65 Oe. At 82 Oe, the degaussed curve is well below the normal ZFC curve. The observed behavior arise due to the fact that the normal ZFC and degaussed state are different in terms arrangement and size of domains even though the net dipole moment is zero in zero field (before the measuring field is applied). At 85 K, when a high field is applied, it results in the formation of large domains, which are broken into smaller pieces by external perturbation (degaussing). Hence, the resultant domain size and arrangement are different from that obtained for normal ZFC at 85 K. So, when the measuring field is applied after ZFC and DG, it leads to different domain size for each case, resulting in the observed difference in temperature response of magnetization between them. This behavior vividly demonstrates inhomogeneous nature of magnetic state, which is not in equilibrium due to the reformation of domains. Many metastable configurations are present within which the wall can make thermally activated hops. When the sample is degaussed after a high field was applied, it results in the formation of the subvalleys with the moments being locked in certain regions and directions. So, measurement at different dc fields after degaussing shows different behaviors for each field when compared with normal ZFC measurements, indicating a hierarchical organization of energy landscape[37] which is discussed in detail later.

B. Suppression of orbital domains and establishment of ferromagnetic long-range order by nonstoichiometry in S2 sample

Figure 4(a), shows the temperature dependence of χ^R in different fields of S2 sample. It clearly shows paramagnetic (PM) to FM transition with the absence of any further transition at low temperature. The absence of strong field dependence indicates the presence of long-range ferromagnetic ordering where domain wall dynamics in an infinite ferromagnetic matrix plays a significant role in defining physical properties of the compound. More vivid manifestation of the role of the walls is emphasized in the inset of Fig. 4(a), which shows the frequency dependence of χ^R. The increase in χ^R with the increasing frequency is an intriguing aspect because χ^R is expected to decrease with the increasing frequency, as observed for metastable systems. In general,

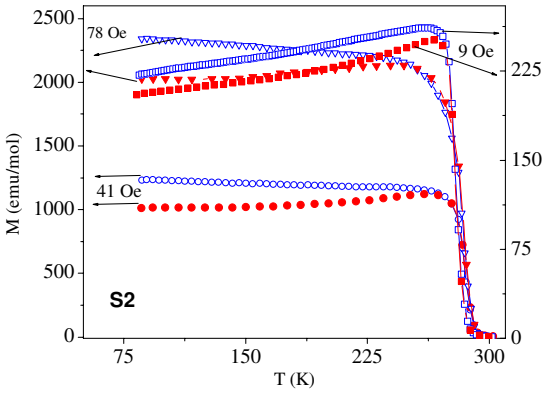

FIG. 5. (Color online) Temperature response of magnetization after zero field cooling (ZFC) (open symbols) and applying a field and degaussing the ZFC sample (closed symbols) at different magnetic fields for S2 sample.

the wall distributions for these types of samples are not in equilibrium and are located in position corresponding to the local potential minima around the pinning centers and oscillate around these metastable position in response to small ac field. Time dependence measurement of susceptibility performed on $LaMnO_{3.075}$ shows that χ^R decreases with time faster for lower frequencies than at higher frequencies below T_c.[38] This implies that walls in a given time stabilize more for a lower frequency than for higher frequency. Moreover, the energy of excitation by the of ac field is proportional to the square of its frequency. So, higher frequency might provide extra perturbation to the pinned walls for depinning, resulting in larger response of spins with increasing frequency. Hence, the observed field and frequency dependences are quite in contrast to that of S1 where systematic frequency and strong field dependence is observed which is ascribed to the distribution of cluster size with the whole clusters being affected by field and frequency change.

To further highlight the role of the domain wall in S2, thermal hysteresis (TH) in ac-χ is performed. The PM to FM transition is second order in nature and hence it is expected that TH to be absent. TH is not observed in χ^R [inset of Fig. 4(b)] as it is dominated by the volume response of the domains and is much less sensitive than imaginary part (χ^I) to the domain wall dynamics. However, a clear difference is seen in the heating and cooling cycles of χ^I [Fig. 4(b)] which arises out of domain wall motion in the low field regime. The difference in temperature cycle of χ^I (which corresponds to the magnetic losses) indicates thermally irreversible domain wall dynamics due to low field irreversible domain wall pinning in the sample. The TH in χ^I disappears (not shown) in the presence of superimposed dc field as the superimposed field is expected to suppress the wall dynamics, emphasizing the above fact that the observed hysteresis is due domain wall motion.

DG measurements performed on the S2 sample shows no change in nature of temperature response of magnetization at different dc fields between the normal curve and the curve noted after degaussing (Fig. 5), with the DG curve always lying below the normal curve. The difference between the curves (Fig. 3 vs Fig. 5) substantiates the fact that the observed features of S2 is only due to the wall dynamics unlike S1 where the domains as a whole is affected by the above protocol.

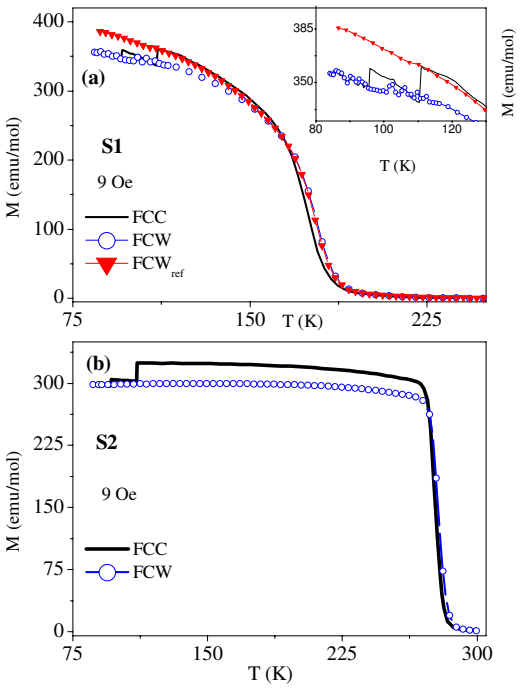

FIG. 6. (Color online) (a) M-T curves during field cooling. The field is switched off at two temperatures (110 and 95 K) for a waiting time of 7200 s. The M-T curve in warming mode and normal FCW curve (as FCW$_{ref}$) is also shown. Inset shows the above graphs up to 125 K. (b) Above protocol (only FCC and FCW) for S2 sample.

Hence, even though both the samples show ferromagnetic behavior, there is a changeover from an orientationly random cluster arrangement of the S1 sample into a homogeneous ferromagnetic ordering for the S2 sample. Hence, it may be considered that the S1 sample is constituted of magnetic clusters which are in a metastable state. The interaction among the clusters results in a glassy state which is responsible for nonequilibrium nature of the low temperature region. The S2 sample consists strongly of coupled regions of equilibrated domains whose once developed correlation are hard to destroy when the temperature is changed. Such behavior is similar to that of low-doped cuprates where there is a competition between the striped and superconducting phases with the change in oxygen stoichiometry.[15]

C. Observation of glassy ferromagnetism in S1 sample and stable ferromagnetism in S2 sample

As stated earlier, the orbital domain state realized in S1 sample results in segregation of charge making the low temperature region inhomogeneous. To further substantiate the inhomogeneous nature and also to get a better insight about the underlying nature of low temperature magnetic ground state of the compound, time dependent magnetization studies under various heating and cooling protocols have been performed. Figure 6(a) shows one such protocol under field

cooled cooling and warming condition. Here, the temperature response of magnetization is noted during FCC from room temperature in 9 Oe magnetic field with temporary stops at 110 and 95 K for a waiting time of 7200 s. During the waiting time, the field is switched off. After each stop at waiting temperatures, the field is reapplied and cooling is restarted. FCW curve is noted immediately after the cooling cycle. Decay in magnetization (aging affect) is observed at the waiting temperatures in FCC mode. Instead of memory of aging, significant fluctuation in magnetization obtained in the warming cycle up to 115 K. To cross-check the fluctuation immediately after the warming cycle, the sample is again cooled in 9 Oe from room temperature to 85 K without any stop and a FCW measurement is done. In this case, the FCW curve [FCW_{ref} in Fig. 6(a)] is smooth with the absence of any fluctuation, indicating that the fluctuation is intrinsic to the sample and is not because of the measuring instrument. It may be noted that in ferromagnetic phase, memory effect is absent during reheating as it is erased by growth of ferromagnetic domains, whereas for a spin glass phase, memory of aging can be observed during heating.[39] Hence, the absence of memory in our case rules out the coexistence of spin glass behavior with ferromagnetic state (i.e., reentrant spin glass phase) at lower temperature. In FCC measurement with stopping, it is seen that aging makes the system stiffer with time resulting in lesser response of the spins with field. Fluctuation obtained in the field cooled warming run indicates that domain wall jumps, as the temperature is swept.[38] Actually, the material being inhomogeneous randomly distributed pinning centers prevents the domain wall from establishing the equilibrium position. Hence, the above measurements give definite evidence that the low temperature region of the compound is inhomogeneous and is not in a state of global minimum.

The above aging measurement performed on S2 sample is shown in Fig. 6(b). Aging effect is observed at the waiting temperatures of 110 and 95 K with the effect being more prominent at the higher temperature. This indicates waiting at 110 K which lead to stabilization of dynamics of the domain walls, resulting in lesser prominence of the effect at 95 K. During the warming cycle, no memory effect of the waiting temperatures is observed, as expected in a ferromagnetic phase. Also, the absence of magnetic fluctuation in warming cycle indicates the stable nature of the low temperature phase of this sample as compared to that of S1.

To further investigate the effect of aging, the waiting time (t_w) dependence of ZFC thermoremanent magnetization (TRM) of both the samples is studied. Figure 7(a) shows M vs t measured with different t_w=1800, 7200, and 10800 s before the application of magnetic field at 95 K. As observed, magnetization clearly depends on the waiting time with M value, decreasing with the increasing t_w for S1 sample. The behavior is obvious, as with increasing t_w, the system becomes stiffer as if the system sinks in deeper and deeper energy valley as time elapses, resulting in lower value of the measured M. In contrasts, even though aging is observed for the S2 sample, M vs t behavior is independent of t_w [inset of Fig. 7(a)] as this sample is more ordered than S1.

For gaining further insight about the underlying nature of the magnetic phase of the samples, low field TRM measure-

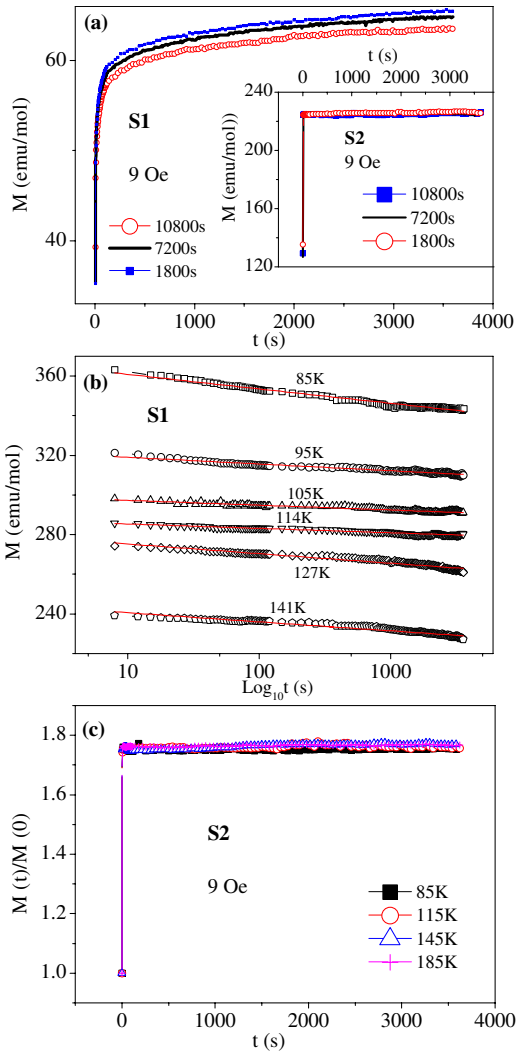

FIG. 7. (Color online) (a) M vs t plot of S1 sample at 95 K for different waiting times (t_w). Inset shows the same measurement for the S2 sample. (b) M is plotted against log t (in s) for S1 sample at different temperatures. The solid lines are best fit to Eq. (1). (c) Normalized magnetic moment $M(t)/M(0)$ is plotted against time for S2 sample after zero field cooling to the measurement temperature and switching on the field.

ments are performed. Figure 7(b) shows the time dependence of magnetization of the S1 sample at different temperature under field cooled (FC) conditions. For each case, the sample is cooled from 250 K in 9 Oe to the measurement temperature where after waiting for 2 min, the field is switched off and magnetization decay is noted. Among the various functional forms that have been proposed to describe the change of magnetization with time, the one proposed by Ulrich *et al.*,[40]

$$M(t) = M_0 t^{-\gamma}, \tag{1}$$

gave good results of fits, while the other functional form yielded unphysical value of constants with large error bars. In the equation, M_0 is related to intrinsic ferromagnetic component and the exponent γ depends on the strength of magnetic interaction. The values of the parameters for S1 are

TABLE I. Values of fitting parameters M_0 and γ of Eq. (1) for sample S1.

T (K)	M (emu/mol)	γ (10^{-3})
85	368.4 ± 0.15	8.9 ± 0.06
95	322.5 ± 0.1	4.0 ± 0.05
105	299.8 ± 0.1	3.5 ± 0.07
114	287.6 ± 0.07	3.4 ± 0.04
125	280.2 ± 0.17	7.7 ± 0.01
141	245.3 ± 0.15	8.0 ± 0.04

complied in Table I. As expected, the value of M_0 increases with the decreasing temperature as field cooled magnetization value increases with decreasing temperature but γ decreases up to 114 K and then increases again. Generally, for glassy systems, the exponent (γ) lies between 0 and 1 and also, in our case, the value of γ lying between the mentioned limits indicating a weak intercluster interaction. For spin glasses or a system of interacting particles with fixed size and concentration, γ is expected to be constant with temperature. The variation in the value of γ as observed is ascribed to the variation of cluster size with temperature, indicating that the cluster size is very fragile to temperature change. This indicates a distribution of potential barrier over which the cluster magnetization tends to relax. The value of γ being lower around 105–114 K is also another signature of the occurrence of orbital rearrangements in the sample.

For S2 sample, ZFC TRM measurements are done where the field is turned on at the measuring temperature after cooling it from room temperature [Fig. 7(c)]. After the field is switched on, magnetization shows a sudden increase in value followed by a very slow increase over the measurement time. TRM (normalized with respect to M value at $t=0$) at different temperatures almost superimposes on each other, indicating that the relaxation at different temperature is almost the same. Good results are not obtained when the curves are fitted by the available functional form that have been proposed to describe the change of magnetization with time, indicating that the growth is neither exponential nor logarithmic.

The nature of the phase in regions where nonequilibrium glassy behavior is observed is generally described either in terms of droplet model[41] or in terms of hierarchical model. The droplet model introduces the concept of overlap length ($L_{\Delta T}$), which determines the maximum length scale at which the spin correlation at two different temperatures (the temperatures being less than spin glass transition temperature) is the same. This characteristic length for the group of spins only at distances larger than $L_{\Delta T}$ is sensitive to small temperature changes. Thus, restart of domain growth is observed from the size $L_{\Delta T}$ not only after cooling but also after heating implying a symmetrical behavior with respect to positive and negative temperature cycle. In this model, it is believed that, at any given temperature below spin glass transition, there is only one phase (and its spin reversed counterpart) to be considered. Hence, it can be said that the energy landscape in this case is dominated by one large valley unlike for hierarchical model, where a multivalley structure is hierarchically organized on the free energy surface. Here, the free energy landscape consists of many local minima corresponding to metastable configuration, which splits into new state when temperature decreases and merges back when the temperature is raised. Hence, hierarchical picture predicts that relaxation is fully initialized on heating implying a nonsymmetrical behavior with respect to heating and cooling unlike the droplet model. Hence, a series of TRM measurement with temperature change as proposed by Sun *et al.*[42] is performed to associate the energy distribution at low temperature phase of the samples with one of the above defined models. The relaxation measurement for sample S1 is shown in Fig. 8(a). The sample is cooled from 240 to 95 K in 0 Oe or 9 Oe field. At 95 K, after waiting for 120 s, the field was switched on or off and magnetization is noted for time t1=1 h. The sample was then cooled in constant and/or zero field to 85 K and TRM is measured for time t2=1 h. Then, the sample was heated back to 95 K in constant/zero field and TRM was measured for time t3=1 h. For the ZFC case, during t1, the curve shows an immediate rise followed by steady growth after the field is switched on. During temporary cooling, the relaxation is weak. Again, when the temperature is raised to 95 K, the magnetization start from the value it reached at the end of t2 indicating the absence of reinitialization after the cooling cycle. For the FC case, magnetization shows an immediate fall followed by steady decay after the field is switched off. During temporary cooling magnetization starts

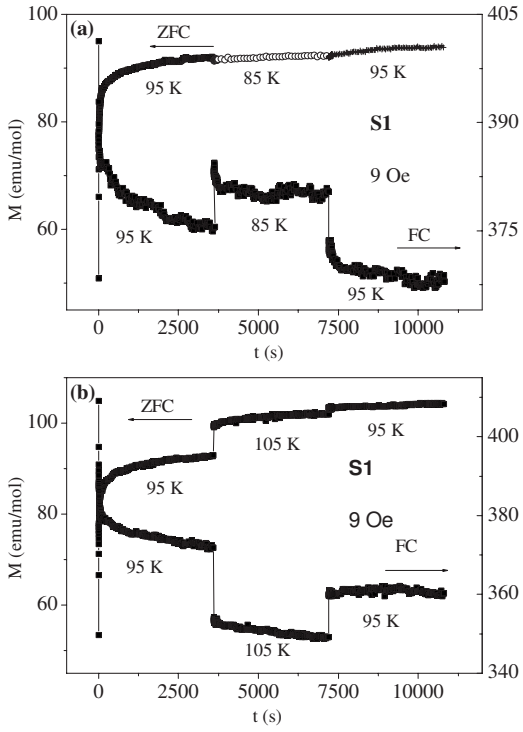

FIG. 8. (a) Magnetic relaxation with temporary cooling for both ZFC (t1, t2, and t3 for 1 h each) and FC (t1, t2, and t3 for 1 h each) cases for S1 sample. (b) Magnetic relaxation with temporary heating for both ZFC (t1, t2, and t3 for 1 h each) and FC (t1, t2, and t3 for 1 h each) cases for S1 sample.

from a higher value but the relaxation is weak. During t3, the relaxation curve starts from a level which is near to the value reached at the end of t1. Figure 8(b) shows the above protocol in the heating cycle where the relaxation curves are noted at 95, 105, and 95 K for times t1, t2, and t3 (1 h each), respectively. Every time the starting value of magnetization is different from the value, it reached at the end of previous TRM measurement. Hence, a clear reinitialization in the relaxation is observed during temporary heating in both ZFC and FC cases. Therefore, it can be said that there is an antisymmetric, response with respect to positive and negative temperature changes in TRM measurement in both ZFC and FC processes which favors a hierarchical picture of energy landscape in the low temperature region which have also been suggested in the earlier section. Interestingly, such picture of energy landscape has also been proposed for many compound such as interacting magnetic nanoparticle system,[42] reentrant systems,[39] etc. The collective interactions of the self-generated assembly of clusters in the low temperature ferromagnetically inhomogeneous phase in our case may give rise to a glassy magnetic behavior which constitute a new class of glass different from conventional spin glass, as also reported in Ref. 43.

The above procedure is performed for sample S2 by cooling it from room temperature, as shown in Figs. 9(a) and 9(b). In this case, the change of magnetization with time is very small and the observed minor change in relaxation behavior during t2 and t3 is only due to change in magnetization value with temperature change. So, the energy landscape of magnetic phase of S2 cannot be ascribed to any of the above models.

IV. CONCLUSION

In summary, we have tried to solve the controversy related to the magnetic ground state in low-doped manganite systems through bulk magnetic measurements on $La_{0.9}Sr_{0.1}MnO_3$. Such systems show a well defined paramagnetic-ferromagnetic transition with the decrease in temperature which falls into the isotropic 3D Heisenberg universality class. However, with further decrease in temperature, there is a sharp change in magnetic susceptibility which is attributed to inhomogeneous ferromagnetism. This inhomogeneity is considered to be arising from the formation of orbital domain state (comprising of ferromagnetic insulating domains separated by ferromagnetic metallic walls), resulting from a discontineous change of lattice parameters at low temperature. This self-organized regimes show metastability which is different from that arising from broad first order phase transitions. It is clearly shown that the low temperature phase shows glassy behavior which is different from conventional spin glass, cluster glass, or dynamics observed in reentrant systems. This glassy phase shows aging affect but no memory and the energy landscape of the degenerate ground state follows the picture of hierarchical model.

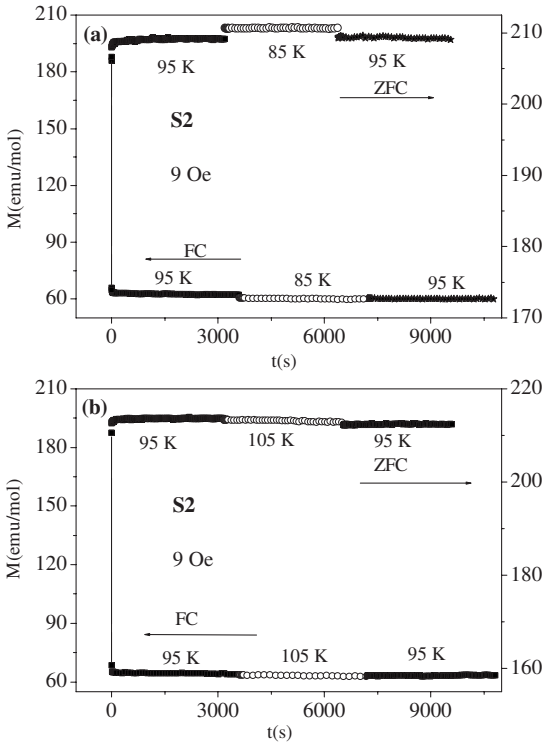

FIG. 9. (a) Magnetic relaxation with temporary cooling for both ZFC (t1, t2, and t3 for 50 min each) and FC (t1, t2, and t3 for 1 h each) cases for S2 sample. (b) Magnetic relaxation with temporary heating for both ZFC (t1, t2, and t3 for 50 min each) and FC (t1, t2, and t3 for 1 h each) cases for S2 sample.

To conclusively assert the fact that the orbital degrees of freedom of the e_g electrons plays an important role in defining the ground state of the system, nonstoichiometry is introduced. Disorder in form of self-doping reduces the Mn^{3+} and hence e_g electrons by 17% in the $La_{0.9}Sr_{0.1}MnO_{3.08}$ sample. This leads to complete destruction of orbital domain state of the stoichiometric sample, resulting in homogeneous ferromagnetic ordering. The ferromagnetic phase of this nonstoichiometric sample does not show glassy behavior and the energy landscape picture of the sample is neither in accordance with hierarchical model or droplet model. Further studies on stoichiometric sample in terms of coupling of spin, orbitals with lattice degrees of freedom, and their dynamics will be useful in understanding the observed unusual glassy behavior of the system. These studies will be important in establishing analogy between self-organized regimes of low-doped manganites with that of cuprates and nickalates.

ACKNOWLEDGMENTS

We are grateful to P. Chaddah for many fruitful discussions. We are thankful to K. Kumar and A. K. Pramanik for help rendered during the course of measurement. K.M. acknowledges CSIR, India for financial support.

[1] H. Kawano, R. Kajimoto, M. Kubota, and H. Yoshizawa, Phys. Rev. B **53**, 2202 (1996).
[2] Y. Yamada, O. Hino, S. Nohdo, R. Kanao, T. Inami, and S. Katano, Phys. Rev. Lett. **77**, 904 (1996).
[3] H. Nojiri, K. Kaneko, M. Motokawa, K. Hirota, Y. Endoh, and K. Takahashi, Phys. Rev. B **60**, 4142 (1999).
[4] Y. Endoh, K. Hirota, S. Ishihara, S. Okamoto, Y. Murakami, A. Nishizawa, T. Fukuda, H. Kimura, H. Nojiri, K. Kaneko, and S. Maekawa, Phys. Rev. Lett. **82**, 4328 (1999).
[5] P. A. Joy and S. K. Date, J. Magn. Magn. Mater. **512**, 196 (2000).
[6] P. A. Algarabel, J. M. De Teresa, J. Blasco, M. R. Ibarra, Cz. Kapusta, M. Sikora, D. Zajac, P. C. Riedi, and C. Ritter, Phys. Rev. B **67**, 134402 (2003).
[7] G. Papavassiliou, M. Pissas, M. Belesi, M. Fardis, J. Dolinsek, C. Dimitropoulos, and J. P. Ansermet, Phys. Rev. Lett. **91**, 147205 (2003).
[8] R. Kajimoto, H. Mochizuki, H. Yoshizawa, S. Okamoto, and S. Ishihara, Phys. Rev. B **69**, 054433 (2004).
[9] J. Geck, P. Wochner, S. Kiele, R. Klingeler, P. Reutler, A. Revcolevschi, and B. Buchner, Phys. Rev. Lett. **95**, 236401 (2005).
[10] K.-Y. Choi, Yu. G. Pashkevich, V. P. Gunezdilov, G. Gntherodt, A. V. Yeremenko, D. A. Nabok, V. I. Kamenev, S. N. Barilo, S. V. Shiryaev, A. G. Soldatov, and P. Lemmens, Phys. Rev. B **74**, 064406 (2006).
[11] Adriana Moreo, Seiji Yunoki, and Elbio Dagotto, Science **283**, 2034 (1999).
[12] Vijay B. Shenoy, Tribikram Gupta, H. R. Krishnamurthy, and T. V. Ramakrishnan, Phys. Rev. Lett. **98**, 097201 (2007).
[13] Sunil Nair and A. Banerjee, Phys. Rev. Lett. **93**, 117204 (2004).
[14] Jan Zaanen and Olle Gunnarsson, Phys. Rev. B **40**, 7391 (1989).
[15] J. H. Cho, F. C. Chou, and D. C. Johnston, Phys. Rev. Lett. **70**, 222 (1993).
[16] J. M. Tranquada, D. J. Buttrey, V. Sachan, and J. E. Lorenzo, Phys. Rev. Lett. **73**, 1003 (1994).
[17] J. M. Tranquada, J. D. Axe, N. Ichikawa, Y. Nakamura, S. Uchida, and B. Nachumi, Phys. Rev. B **54**, 7489 (1996).
[18] J. M. Tranquada, K. Nakajima, M. Braden, L. Pintschovius, and R. J. McQueeney, Phys. Rev. Lett. **88**, 075505 (2002).
[19] T. Mizokawa, D. I. Khomskii, and G. A. Sawatzky, Phys. Rev. B **61**, R3776 (2000).
[20] T. Hotta, Adrian Feiguin, and Elbio Dagotto, Phys. Rev. Lett. **86**, 4922 (2001).
[21] A. Urushibara, Y. Moritomo, T. Arima, A. Asamitsu, G. Kido, and Y. Tokura, Phys. Rev. B **51**, 14103 (1995).
[22] S. Nair, A. Banerjee, A. V. Narlikar, D. Prabhakaran, and A. T. Boothroyd, Phys. Rev. B **68**, 132404 (2003).
[23] V. E. Arkhipov, V. S. Gaviko, A. V. Korolyov, V. E. Naish, V. V. Marchenkov, Ya. M. Mukovskii, S. G. Karabashev, D. A. Shulyatev, and A. A. Arsenov, J. Magn. Magn. Mater. **196**, 539 (1999).
[24] H. Kawano, R. Kajimoto, M. Kubota, and H. Yoshizawa, Phys. Rev. B **53**, R14709 (1996).
[25] T. Sato, T. Ando, T. Ogawa, S. Morimoto, and A. Ito, Phys. Rev. B **64**, 184432 (2001).
[26] A. M. Van Roosmalen, E. H. P. Cordfunke, R. B. Helmholdt, and H. W. Zandbergenet, J. Solid State Chem. **110**, 100 (1994).
[27] M. A. Senaris-Rodriguez and J. B. Goodenough, J. Solid State Chem. **118**, 323 (1995).
[28] Q. A. Li, K. E. Gray, H. Zheng, H. Claus, S. Rosenkranz, S. N. Ancona, R. Osborn, J. F. Mitchell, Y. Chen, and J. W. Lynn, Phys. Rev. Lett. **98**, 167201 (2007).
[29] R. A. Young, A. Sakthivel, T. S. Moss, C. O. Paiva-Santos, *User Guide To Program DBWS-9411* (Georgia Institute of technology, Atlanta, 1994).
[30] A. Bajpai and A. Banerjee, Rev. Sci. Instrum. **68**, 4075 (1997).
[31] R. V. Krishnan and A. Banerjee, Rev. Sci. Instrum. **70**, 85 (1999).
[32] R. S. Freitas, L. Ghivelder, F. Damay, F. Dias, and L. F. Cohen, Phys. Rev. B **64**, 144404 (2001), and references therein.
[33] T. Shibata, Bruce Bunker, J. F. Mitchell, and Peter Schiffer, Phys. Rev. Lett. **88**, 207205 (2002).
[34] J. B. Goodenough, Phys. Rev. **100**, 564 (1955).
[35] R. V. Krishnan and A. Banerjee, J. Phys.: Condens. Matter **12**, 3835 (2000).
[36] G. Zarand, F. Pazmandi, K. F. Pal, and G. T. Zimanyi, Phys. Rev. Lett. **89**, 150201 (2002).
[37] F. Lefloch, J. Hammann, M. Ocio, and E. Vincent, Europhys. Lett. **18**, 647 (1992); E. Vincent, J. P. Bouchaud, J. Hammann, and F. Lefloch, Philos. Mag. B **71**, 489 (1995).
[38] M. Muroi, R. Street, J. W. Cochrane, and G. J. Russell, Phys. Rev. B **64**, 024423 (2001).
[39] E. Vincent, V. Dupuis, M. Alba, J. Hammann, and J. P. Bouchaud, Europhys. Lett. **50**, 674 (2000).
[40] M. Ulrich, J. Garc-a-Otero, J. Rivas, and A. Bunde, Phys. Rev. B **67**, 024416 (2003).
[41] Daniel S. Fisher and David A. Huse, Phys. Rev. B **38**, 373 (1988); **38**, 386 (1988).
[42] Young Sun, M. B. Salamon, K. Garnier, and R. S. Averback, Phys. Rev. Lett. **91**, 167206 (2003).
[43] F. Rivadulla, M. A. Lopez-Quintela, and J. Rivas, Phys. Rev. Lett. **93**, 167206 (2004).